

# In Vitro Comparison of 2 Clinically Applied Biomaterials for Autologous Chondrocyte Implantation: Injectable Hydrogel Versus Collagen Scaffold

CARTILAGE  
2023, Vol. 14(2) 220–234  
© The Author(s) 2023  
DOI: 10.1177/19476035231154507  
journals.sagepub.com/home/CAR

Jan-Tobias Weitkamp<sup>1,2</sup> , Karin Benz<sup>3</sup>, Bernd Rolauffs<sup>4</sup>,  
Andreas Bayer<sup>2</sup>, Matthias Weuster<sup>5</sup>, Ralph Lucius<sup>2</sup>, Aydin Gülses<sup>1</sup>,  
Hendrik Naujokat<sup>1</sup>, Jörg Wiltfang<sup>1</sup>, Sebastian Lippross<sup>6</sup>,  
Michael Hoffmann<sup>7</sup>, Bodo Kurz<sup>2</sup>, and Peter Behrendt<sup>2,7</sup>

## Abstract

**Objective.** In autologous chondrocyte implantation (ACI), there is no consensus about used bioscaffolds. The aim of this study was to perform an *in vitro* comparative analysis of 2 clinically applied biomaterials for cartilage lesion treatment. **Design.** Monolayer expanded human chondrocytes ( $n = 6$ ) were embedded in a collagen scaffold (CS) and a hyaluronic acid–based hydrogel (HA). Cells were cultured in chondropermissive medium supplemented with and without interleukin-10 (IL-10) and bone morphogenetic protein–2 (BMP-2). Gene expression of chondrogenic markers (COL1A1, COL2A1, COL10A1, ACAN, SOX9) was detected *via* quantitative real-time–polymerase chain reaction (RT-qPCR). Biosynthesis of matrix compounds, cell viability, morphology as well as migration from surrounding native bovine cartilage into cell-free scaffolds were analyzed histologically. Adhesion of the material to adjacent cartilage was investigated by a custom-made push-out test. **Results.** The shift of COL1/2 ratio toward COL2A1 was more pronounced in HA, and cells displayed a more spherical morphology compared with CS. BMP-2 and IL-10 significantly increased COL2A1, SOX9, and ACAN expression, which was paralleled by enhanced staining of glycosaminoglycans (GAGs) and type 2 collagen in histological sections of CS and HA. COL10A1 was not significantly expressed in HA and CS. Better interfacial integration and enhanced cell invasion was observed in CS. Push-out tests using CS showed higher bonding strength to native cartilage. **Conclusion.** HA-based hydrogel revealed a more chondrocyte-like phenotype but only allowed limited cell invasion, whereas CS were advantageous in terms of cellular invasion and interfacial adhesion. These differences may be clinically relevant when treating cartilaginous or osteochondral defects.

## Keywords

autologous chondrocyte implantation, collagen scaffold, hydrogel, hyaluronic acid, human articular chondrocytes, *in vitro* comparison

<sup>1</sup>Department of Oral and Maxillofacial Surgery, University Medical Center Schleswig-Holstein, Campus Kiel, Kiel, Germany

<sup>2</sup>Department of Anatomy, Kiel University, Kiel, Germany

<sup>3</sup>TETEC Tissue Engineering Technologies AG, Reutlingen, Germany

<sup>4</sup>G.E.R.N. Research Center for Tissue Replacement, Regeneration & Neogenesis, Department of Orthopedics and Trauma Surgery, Medical Center Albert-Ludwigs-University of Freiburg, Faculty of Medicine, Albert-Ludwigs-University of Freiburg, Freiburg, Germany

<sup>5</sup>Clinic for Trauma Surgery, Diako Hospital Flensburg, Flensburg, Germany

<sup>6</sup>Department of Trauma and Orthopedic Surgery, University Medical Center Schleswig-Holstein, Campus Kiel, Kiel, Germany

<sup>7</sup>Department of Trauma Surgery, Orthopedics and Sportsorthopedics, Asklepios Klinik St. Georg, Hamburg, Germany

## Corresponding Author:

Jan-Tobias Weitkamp, Department of Oral and Maxillofacial Surgery, University Medical Center Schleswig-Holstein, Campus Kiel, Arnold-Heller-Str. 3, Kiel 24105, Germany.

Email: jan-tobias.weitkamp@uksh.de



Creative Commons Non Commercial CC BY-NC: This article is distributed under the terms of the Creative Commons Attribution-NonCommercial 4.0 License (<https://creativecommons.org/licenses/by-nc/4.0/>) which permits non-commercial use, reproduction and distribution of the work without further permission provided the original work is attributed as specified on the SAGE and Open Access pages (<https://us.sagepub.com/en-us/nam/open-access-at-sage>).

## Introduction

Articular cartilage repair remains a challenging task in the field of orthopedic surgery aiming to prevent joint dysfunction and the development of post-traumatic osteoarthritis. Autologous chondrocyte implantation (ACI) has become the gold standard for the regenerative treatment of large size cartilage defects.<sup>1,2</sup> Within the last 3 decades, the originally introduced technique was further developed by utilizing additional biomaterials as cell-carrier systems.<sup>3,4</sup>

Different generations of ACI development have aimed to overcome the issue of chondrocyte de-differentiation, which impairs the chondrocyte function and results in inferior quality of the regenerative tissue.<sup>5</sup> Third-generation ACI consists of a cell-biomaterial product that has improved both the clinical outcome and the histological quality of the regenerated tissue, which emphasizes the constant optimization process of cell-based tissue regeneration techniques.<sup>3,6</sup> Numerous biomaterials have been extensively studied in pre-clinical investigations, but comparative studies are rare. Therefore, identification of the ideal biomaterial candidate regarding its cell-matrix interactions, cytocompatibility, biomechanical properties, and surgical application techniques is insufficient. In addition, due to regulatory restrictions and financial burdens, it is not feasible to examine the whole spectrum of biomaterials clinically. A deepened knowledge about biomaterial advantages in clinically established biomaterials may help to focus current efforts in further ACI development. In this regard, biomaterials based on collagen and hyaluronic acid, which are inspired by the natural architecture of articular cartilage, are of high interest for investigators in this field.<sup>7-9</sup> Fiber-based matrices have shown to support chondrocyte differentiation and formation of cartilaginous matrix in several *in vitro* and *in vivo* studies.<sup>10,11</sup> Hydrogels, on the contrary, have also been investigated intensively due to their water-binding capacity that mimics cartilage tissue.<sup>12</sup> Especially, gels based on naturally derived biopolymers such as hyaluronic acid are interesting for cartilage tissue engineering due to its chondroprotective effects.<sup>13</sup>

Another improvement in ACI treatment may be achieved by a pre-conditioning using soluble adjuvants that improve cell differentiation prior to ACI implantation. In this context, interleukin-10 (IL-10) and bone morphogenetic protein-2 (BMP-2) have been described,<sup>14,15</sup> which were shown to have potential chondrogenic effects, even in the post-traumatic micromilieu after ACI graft transplantation.<sup>16,17</sup> Our study group previously demonstrated that IL-10 significantly enhances chondrogenic differentiation of cells embedded in collagen matrices and stabilized the chondrogenic phenotype with less extracellular matrix loss after mechanical cartilage injury.<sup>14,18</sup> BMP-2, a member of the transforming growth factor- $\beta$  (TGF- $\beta$ ) super-family, plays an essential role in the regulation of chondrocyte proliferation.<sup>15</sup>

Given the abundant spectrum of eligible biomaterials, deepened understanding of clinically applied scaffolds may help to focus further ACI developments. This study aims to identify advantageous biomaterial properties of 2 clinically used ACI grafts (macroporous type I/III collagen matrix vs. injectable hyaluronic acid-based hydrogel) in a comparative *in vitro* study with respect to (1) cell viability, (2) chondrogenic potential, (3) bio-adhesion, (4) lateral integration, and (5) additional adjuvants such as IL-10 and BMP-2. It was hypothesized that both biomaterials have distinct biological differences regarding cell differentiation and graft integration.

## Method

### Articular Chondrocyte Isolation and Culture

Human articular chondrocytes (hCh;  $n = 6$ ) were isolated from femoral heads of patients (mean =  $70.3 \pm 5.3$  years) undergoing hip replacement surgery (ethical approval was obtained of the University Kiel D572/17). The cartilage tissue was dissected into small pieces and digested with 0.1% pronase (Roche, Mannheim, Germany) followed by digestion with type 2 collagenase 600 U/ml (Worthington, Lakewood, USA) in Dulbecco's Modified Eagle Medium (DMEM). Isolated hCh were cultured at a density of 10,000 cells/cm<sup>2</sup> in chondropermissive medium (CPM) consisting of high-glucose DMEM (HG-DMEM) supplemented with 10% Sera Plus (PAN-Biotech, Aidenbach, Germany), 10 mg/ml Penicillin G, 10 mg/ml of streptomycin (PAA Laboratories, Pasching, Germany), 1% L-ascorbic acid (Sigma-Aldrich, St. Louis, USA) and 2 ng/ml fibroblastic growth factor-2 (FGF-2; R&D Systems, Minneapolis, USA). Medium change was twice a week. Cells were harvested at cell passage 3 (P3) by trypsin-ethylenediaminetetraacetic acid (EDTA; Lonza, Cologne, Germany) treatment and used for further *in vitro* cultivation.

### Embedding of hCh in HA and CS

Monolayer expanded chondrocytes (P3) ( $n = 6$ ) were seeded either onto the macroporous part of a biphasic type 1/3 collagen scaffold (CS) as used in Novocart 3D® (TETEC Tissue Engineering Technologies AG, Reutlingen, Germany) or were embedded in an albumin-hyaluronic acid-based hydrogel (HA) as used in Novocart Inject® (TETEC Tissue Engineering Technologies AG, Reutlingen, Germany). Therefore,  $2.5 \times 10^6$  hCh/ml/cm<sup>2</sup> were re-suspended in HG-DMEM and seeded onto the CS and HA, respectively, and cultivated in 24-well plates coated with 2% agarose (Sigma-Aldrich, St. Louis, USA). The hydrogel is based on chemically activated maleolyl-albumin supplemented with HA and was cross-linked by a specific thio-polyethylene glycol (PEG).<sup>13</sup>

**Table 1.** Human Primer Sequences (5'-3').

Human Target	Sequence (5'-3')
ACAN sense	GAGGCCAGCAGAGAAGATTCTG
ACAN antisense	GACGCCTCGCCTTCTTGAA
COL2A1 sense	CAACACTGCCAACGTCCAGAT
COL2A1 antisense	CTGCTTCGTCCAGATAGGCAAT
SOX9 sense	CTCGGAGACTTCTGAACGAGAG
SOX9 antisense	CGTTCTTCACCGACTTCCTCC
COL1A1 sense	AATTCCAAGGCCAAGAAGCATG
COL1A1 antisense	GGTAGCCATTTCCTTGGTGGTT
COL10A1 sense	CCCTTTTGTGCTGCTAGTATCCTTGA
COL10A1 antisense	AACTGTGTCTTGGTGTGGGTAGTG
GAPDH sense	GCCTCAAGATCATCAGCAATGC
GAPDH antisense	TGGTCATGAGTCCTTCCACGAT

ACAN = human aggrecan; COL2A1 = type 2 collagen; SOX9 = transcription factor SOX-9; COL1A1 = type 1 collagen, COL10A1 = type 10 collagen; GAPDH = glyceraldehyde 3-phosphate dehydrogenase.

Cellularized constructs were cultured in CPM (without Sera Plus) that was supplemented with 1% insulin-transferrin-sodium selenite liquid media (Sigma-Aldrich, St. Louis, USA) and 0.1 mM nonessential amino acids (Sigma-Aldrich, St. Louis, USA) and renewed every 3 days. The samples were divided into 4 different treatment groups: non-supplemented, additional human IL-10 (100 pg/ml; Kingfisher Biotech, Saint-Paul, USA), additional human bone morphogenetic protein-2 (hBMP-2; 250 ng/ml; R&D Systems, Minneapolis, USA), and co-treatment with IL-10 and BMP-2.

### Cell Viability, Morphology, and Expression of Microfiber Assessment

To determine the morphology and viability of cells within the biomaterial live/dead (L/D), staining was performed after 7 and 28 days of culture. Therefore, HA and CS samples were stained with 10  $\mu$ M calcein-AM and 5  $\mu$ M ethidium homodimer-1 (both Sigma-Aldrich, Buchs, Switzerland). After 1-hour incubation, the samples were imaged using confocal laser scanning microscopy (CLSM 510; Carl Zeiss, Germany). To quantify the number of L/D cells, 3 images were taken from 3 different fields of view, and a minimum of 100 cells were counted using image J (Wayne Rasband, NIH, USA). To visualize the expression of F-actin, additional staining with phalloidin and nuclear staining (4',6-diamidino-2-phenylindole [DAPI]) was performed followed by CLSM.

### Gene Expression Analyses by Quantitative Real-Time PCR

Gene expression was analyzed after 1 and 28 days. HA samples were pre-digested with proteinase K (3 mg/ml in

HG-DMEM; Roche, Germany). Total RNA of the digest of HA and CS samples was extracted using the RNeasy Mini Kit according to the manufacturer's instructions (Qiagen, Hilden, Germany). Complementary DNA was obtained by reverse transcription using Qiagen RT-PCR Kit (Qiagen, Hilden, Germany). Quantitative real-time-polymerase chain reaction (RT-qPCR) was performed using glyceraldehyde-3-phosphate dehydrogenase (GAPDH) as the reference gene and Qiagen QuantiTect SYBR® Green RT-PCR Kit according to manufacturer's instructions with a 7500 Fast Real-Time PCR System (Applied Biosystems, Darmstadt, Germany). Human aggrecan (ACAN), type 2 collagen (COL2A1), transcription factor SOX-9 (SOX9), type 1 collagen (COL1A1), type 10 collagen (COL10A1), and GAPDH (all Biomers, Ulm, Germany) primers were used at a concentration of 0.3  $\mu$ M (Table 1). Data analysis was performed using a comparative quantification ( $\Delta\Delta$ CT-method). Untreated monolayer (P4) served as control group.

### DNA Quantification and DMMB-Assay

After 28 days, CS and HA samples ( $n = 3$ ) digested with 0.5 mg/ml proteinase K (Roche, Mannheim, Germany). Sulphated glycosaminoglycans (sGAG) content within the digest and the cumulative supernatant was detected with modified 1,9-dimethylmethylene blue (DMMB) assay (Sigma-Aldrich, Darmstadt, Germany) according to Zheng and Levenston.<sup>19</sup> The DNA content of the digest was quantified using a bisbenzimidazole-based DNA quantification assay according to manufacturer's protocol (Promega, Mannheim, Germany).

### Histology Studies

After 28 days, samples were mounted in tissue compound and cryo-sectioned (thickness: 10  $\mu$ m) using Microm HM 56Cryostat-Microtome (Carl Zeiss AG, Zürich, Switzerland). CS and HA samples were stained with toluidine blue according to standard protocol.<sup>20</sup> Immunohistochemistry (IHC) of type 2 collagen (mouse anti-type-II-collagen antibody; Clone ClIC1, DSHB, Iowa, USA; as described in) and type 1 collagen (mouse anti type-I-collagen antibody; C-2456 Sigma-Aldrich) was performed as described in Gille et al.<sup>21</sup> and Kurz et al.<sup>22</sup>

### Preparation of Bovine Cartilage Plugs and Invasion Assay

Cartilage cylinders of bovine stifle joints were harvested as described before.<sup>23</sup> The defect was filled with cell-free HA and CS ( $n = 6$ ). Agarose 2% (Lonza, Basel, Switzerland) served as negative control. Chondrocyte invasion from a bovine cartilage into the embedded biomaterials was analyzed using CLSM (as described above) after 28

days cultivation time. The plugs were cultivated in an 2% agarose coated 24-well plate with CPM. For quantification of cell invasion in %, the total area of embedded biomaterials was divided into 100 equal areas. Using image J, areas colonized with cells were counted. Images of  $n = 6$  were used to quantify cell invasion in CS, HA, and agarose.

### Investigations of the Biomaterial/Tissue Interface

To determine the bonding strength of HA and CS to native cartilage tissue, push-out tests were performed as described before.<sup>23</sup> For the push-out test, the defect was filled with HA and CS (without and with  $2.5 \times 10^6$  hCh/ml/cm<sup>2</sup>) or 2% agarose (Lonza, Basel, Switzerland) as negative control. Tissue/scaffold constructs were cultured in CPM for up to 28 days. The mechanical test was performed with 6 cartilage rings for each condition and repeated using the cartilage rings isolated from 3 different animals. The bonding strength was calculated by dividing the loading peak (N) by the bonding area (m<sup>2</sup>).

### Biomechanical Testing: Young's Modulus

Biomechanical tests were carried out in a standard material-testing machine (Instron 5866 electromechanical test device) equipped with a 10 N load cell. The initial sample height  $h_0$  was measured with a caliper and samples placed in a cell culture dish filled with chondrogenic medium. A 1-step unconfined compression test was performed by loading the sample through a flat-ended indenter (0.02 N preload) at a strain rate of 0.5 mm/min until 50%  $h_0$  strain was reached. The Young's modulus was then calculated at the initial linear part of the stress-strain-curve ( $n = 6$ ).

### Statistics

All data were tested for normality using the Kolmogorov–Smirnov test. Statistical analysis was performed using Graph Pad prism 5 program (San Diego, CA, USA). One-way analysis of variance (ANOVA) with Bonferroni's multiple comparison was used to compare means among the independent experimental groups. Differences were considered significant if  $P \leq 0.05$ . Quantitative data in the text are presented as mean and standard deviation (SD).

## Results

### Both Biomaterials Support High Cell Viability

Detection of metabolic cell activity at day 1 and day 28 showed similar results for hCh seeded in both biomaterials. Relative fluorescence units increased significantly from day 1 to day 28 in non-supplemented and IL-10 supplemented HA and CS (HA day 1 vs. day 28:  $P = 0.0004$ ; HA + IL-10 day 1 vs. day 28:  $P = 0.0176$ ; CS day 1 vs. day 28:  $P = 0.0005$ ; CS

+ IL-10 day 1 vs. day 28:  $P < 0.0001$ ; **Figure 1a(A)**). The presence of BMP-2 led to an initial significant increase of metabolic cell activity in both biomaterials at day 1 (HA vs. HA + BMP-2 and HA vs. HA + BMP-2 + IL-10 day 1:  $P < 0.0001$ ; CS vs. CS + BMP-2 and CS vs. CS + BMP-2 + IL-10 day 1:  $P < 0.0001$ ; **Figure 1a(A)**).

Cell quantification of live and dead cells revealed a high proportion of viable hCh in HA and CS during 4 weeks of *in vitro* cultivation (HA day 1:  $93\% \pm 1.76\%$ ; CS day 1:  $84.33\% \pm 8.48\%$ ; **Figure 1a(B)**). At day 28, significantly more viable hCh were detected in HA ( $P = 0.0006$ ), but still more than  $74\% \pm 8.85\%$  hCh were viable in CS. Supplementing BMP-2 and IL-10 had no significant influence on cell viability (data not shown).

Morphologically, hCh embedded in hydrogel showed a spherical phenotype in contrast to a fibroblastic-like cell phenotype in the 3D collagen matrix (**Fig. 1b(A1 and C1)**). The ramified cell phenotype was paralleled by greater F-actin accumulation in cells embedded in CS (**Fig. 1c(A and B)**).

### Chondrocytes in Hydrogel Show Superior Chondrogenic Re-Differentiation

Cells cultivated in CPM showed a time-dependent increase of chondrogenic marker expression in both biomaterials (**Fig. 2(A-F)**), except COL2A1 in untreated HA. Cell re-differentiation was strongly enhanced by BMP-2 treatment, while supplementation of IL-10 was less effective. Overall, a trend for marked chondrogenic marker expression was observed in the hydrogel groups as demonstrated by shift from COL1A1 to COL2A1 (**Fig. 2(F)**).

In detail, BMP-2 supplementation significantly increased relative gene expression of COL2A1 in HA by 3.4 ( $P = 0.0039$ ; **Fig. 2(A)**). After 28 days, significantly increased COL2A1 expression was detected in those experimental groups that had received the addition of BMP-2 and the co-treatment of IL-10 and BMP-2 (HA day 28 vs. HA + BMP-2 day 28:  $P < 0.0001$ ; HA day 28 vs. HA + BMP-2 + IL-10 day 28:  $P < 0.0001$ ). For CS groups, a comparable COL2A1 induction was observed but the expression levels remained significantly lower compared with the hydrogel groups (HA + BMP-2 day 28 vs. CS + BMP-2 day 28:  $P < 0.0001$ ). Transcription levels of ACAN showed a comparable pattern (**Fig. 2(B)**). In HA groups, relative mRNA expression was significantly amplified under BMP-2 treatment (HA day 28 vs. HA + BMP-2 day 28:  $P = 0.0002$ ; HA day 28 vs. HA + BMP-2 + IL-10 day 28:  $P < 0.0001$ ) and was also significantly higher than of CS groups after 28 days (HA + BMP-2 day 28 vs. CS + BMP-2 day 28:  $P = 0.0004$ ). For SOX9, mRNA expression tended to be higher in HA groups without significant effects of IL-10 and BMP-2 (**Fig. 2(C)**). Furthermore, there was a trend for lower mRNA



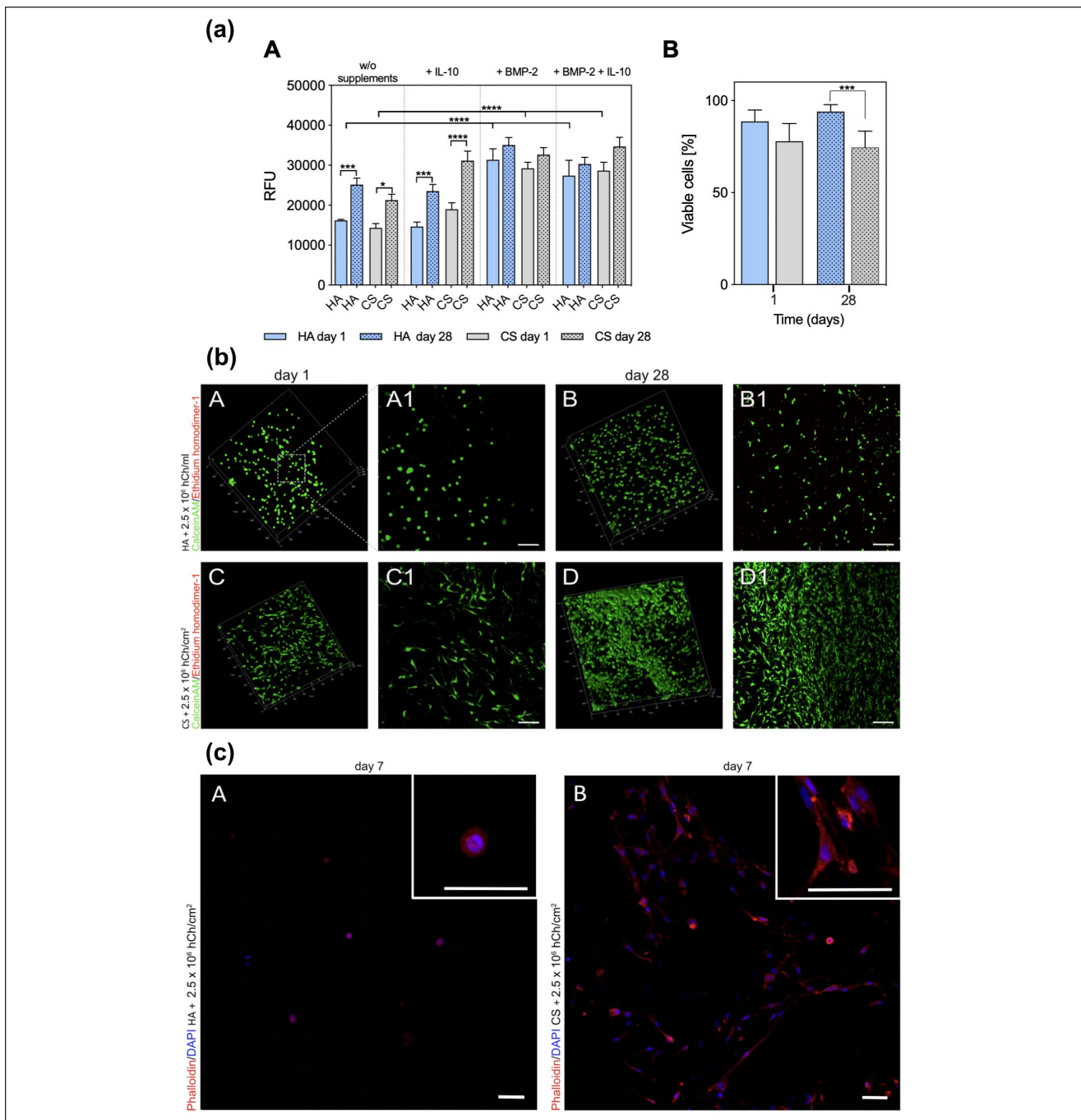


**Figure 1.** (a) Metabolic cell activity and viable quantification: **(A)** Celltiter-blue assay of hChs embedded in HA and CS after 1 and 28 days with and without supplementation of IL-10 (100 pg/ml) and BMP-2 (250 ng/ml). **(B)** Quantification of viable cells (%) after 1 and 28 days. Cells were cultured in chondropermissive medium without IL-10 and BMP-2 supplementation. HA = hyaluronic acid-based hydrogel; CS = collagen scaffold; IL-10 = interleukin-10; BMP-2 = bone morphogenetic protein-2; ANOVA = analysis of variance; SD = standard deviation. Asterisks indicate significant differences with \* $P < 0.05$ , \*\* $P < 0.01$ , \*\*\* $P < 0.001$ , \*\*\*\* $P < 0.0001$ , one-way ANOVA. Data are presented as mean + SD ( $n = 3$ ). **(b)** Chondrocyte viability and morphology in HA and CS: **(A-D)** Representative 3-dimensional reconstructions of cell-laden HA and CS after L/D staining at day 1 and day 28. Cells were cultured in chondropermissive medium without IL-10 and BMP-2 supplementation. An increase in cell density indicates proliferation in both biomaterials. **(A1-D1)** Representative 2-dimensional sections. Chondrocytes in HA appear spheric while cells in CS displayed a ramified phenotype. **(c)** Cytoskeletal changes: Expression of actin stress-fibers. Phalloidin/DAPI staining of human articular chondrocytes embedded in CS **(A)** and HA **(B)** after 7 days of culture in chondropermissive medium **(b and c)**. HA = hyaluronic acid-based hydrogel; CS = collagen scaffold; IL-10 = interleukin-10; BMP-2 = bone morphogenetic protein-2; ANOVA = analysis of variance; DAPI = 4',6-diamidino-2-phenylindole. Bar 25  $\mu$ m

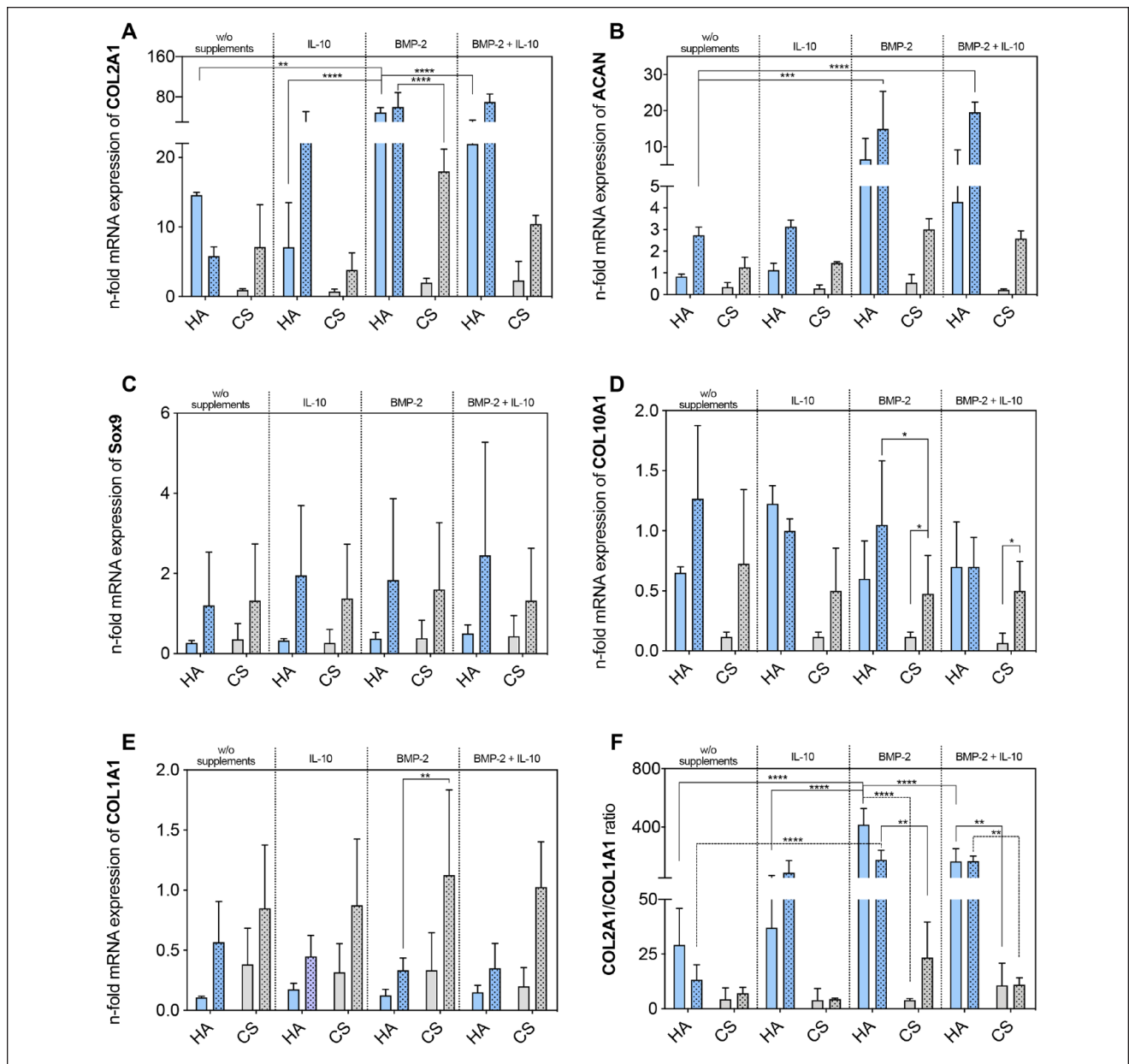


**Figure 2.** Chondrogenic potential of human articular chondrocytes embedded in HA and CS. Transcription levels of messenger ribonucleic acid (mRNA) of chondrogenic markers ((**A**) COL1A1, (**B**) ACAN, (**C**) SOX9) and markers of de-differentiation ((**D**) COL1A1, (**E**) COL10A1) were measured after 1 and 28 days incubation with IL-10 (100 pg/ml), BMP-2 (250 ng/ml), and co-treatment. COL2A1/COL1A1 ratio is displayed in (**F**). Gene expression levels were normalized to that of GAPDH reference gene and then normalized to day 1 monolayer chondrocytes, which had an expression level = 1. HA = hyaluronic acid-based hydrogel; CS = collagen scaffold; COL10A1 = type 10 collagen; ACAN = human aggrecan; SOX9 = transcription factor SOX-9; IL-10 = interleukin-10; BMP-2 = bone morphogenetic protein-2; GAPDH = glyceraldehyde-3-phosphate dehydrogenase; ANOVA = analysis of variance; SD = standard deviation. Asterisks indicate significant differences with \* $P < 0.05$ , \*\* $P < 0.01$ , \*\*\* $P < 0.001$ , \*\*\*\* $P < 0.0001$ , one-way ANOVA. Data are presented as mean + SD ( $n = 3$ ).

expression of the cell de-differentiation marker COL1A1 in untreated HA compared with CS groups (**Fig. 2(E)**). Treatment with BMP-2 led to positive effects by significantly lowering COL1A1 expression levels in HA compared with CS groups after 28 days of culture (HA +

BMP-2 day 28 vs. CS + BMP-2 day 28:  $P = 0.003$ ). The cell hypertrophy marker COL10A1 was similar in HA similar to monolayer chondrocytes but reduced in CS groups (**Fig. 2(D)**).

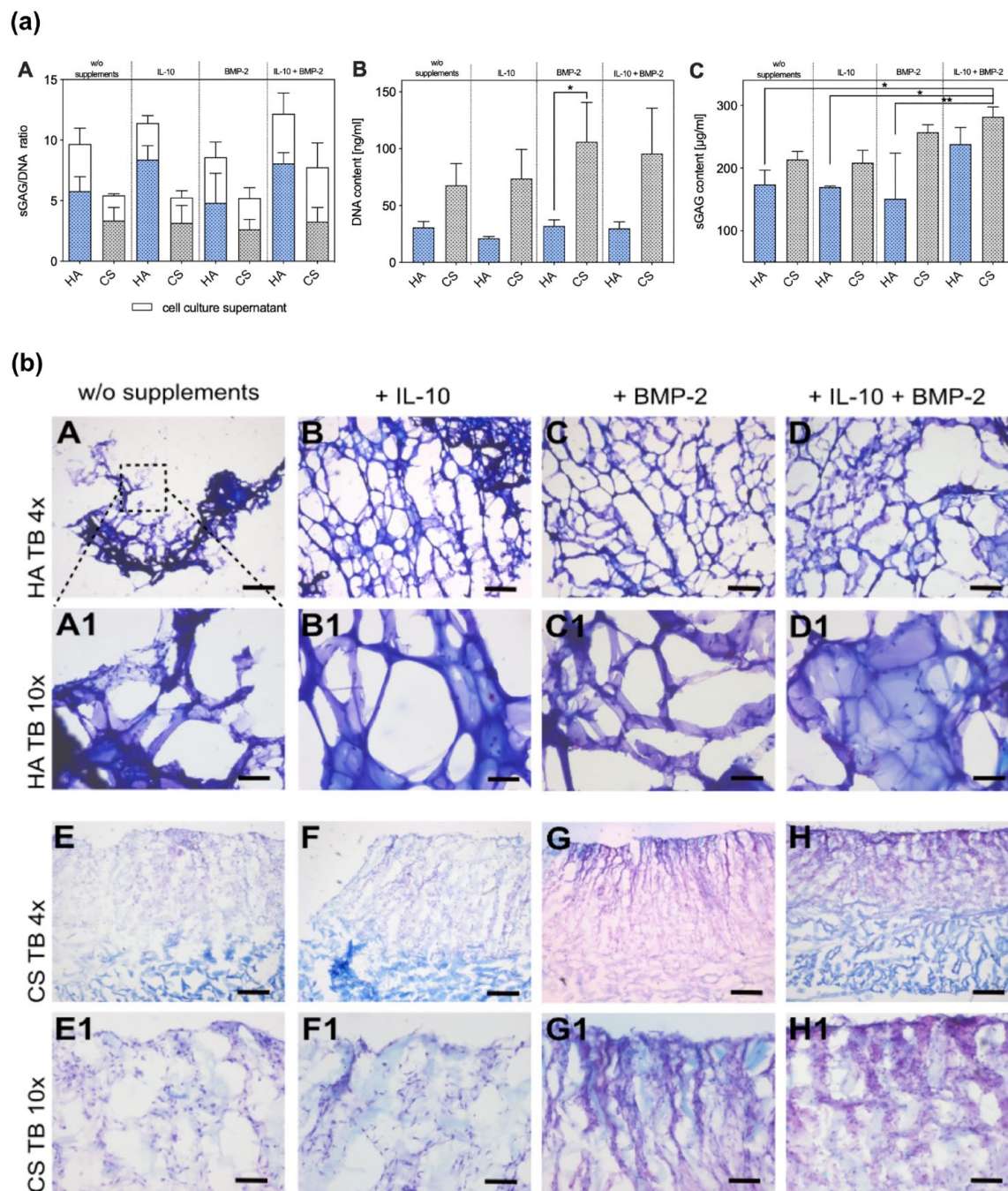


**Figure 3.** (a) Glycosaminoglycan content and release in cell-laden HA and CS normalized to DNA content (**A-C**). Cell-laden biomaterials after 28 days of culture with and without IL-10 (100 pg/ml), BMP-2 (250 ng/ml), and co-treatment, respectively. (**A**) Total sGAG content and cumulative GAG release were analyzed by DMMB assay and normalized to corresponding sample's DNA content (GAG/DNA ratio). (**B**) Total DNA content and (**C**) total sGAG content in HA and CS groups. Asterisks indicate significant differences with  $*P < 0.05$ ,  $**P < 0.01$ , one-way ANOVA. Data are presented as mean + SD ( $n = 3$ ). (b) Glycosaminoglycan biosynthesis in cellularized HA (**A-D**) and CS (**E-H**). Representative images of TB staining after 28 days of *in vitro* culture in chondropermissive medium with and without IL-10 and BMP-2 supplementation (enhanced metachromasia due to acidophilic sGAGs). HA = hyaluronic acid-based hydrogel; CS = collagen scaffold; IL-10 = interleukin-10; BMP-2 = bone morphogenetic protein-2; sGAG = sulphated glycosaminoglycans; DNA = deoxyribonucleic acid; DMMB = dimethylmethylene blue; TB = toluidine blue. Bar 200 μm (**A1-D1, E1-H1**: 100 μm).



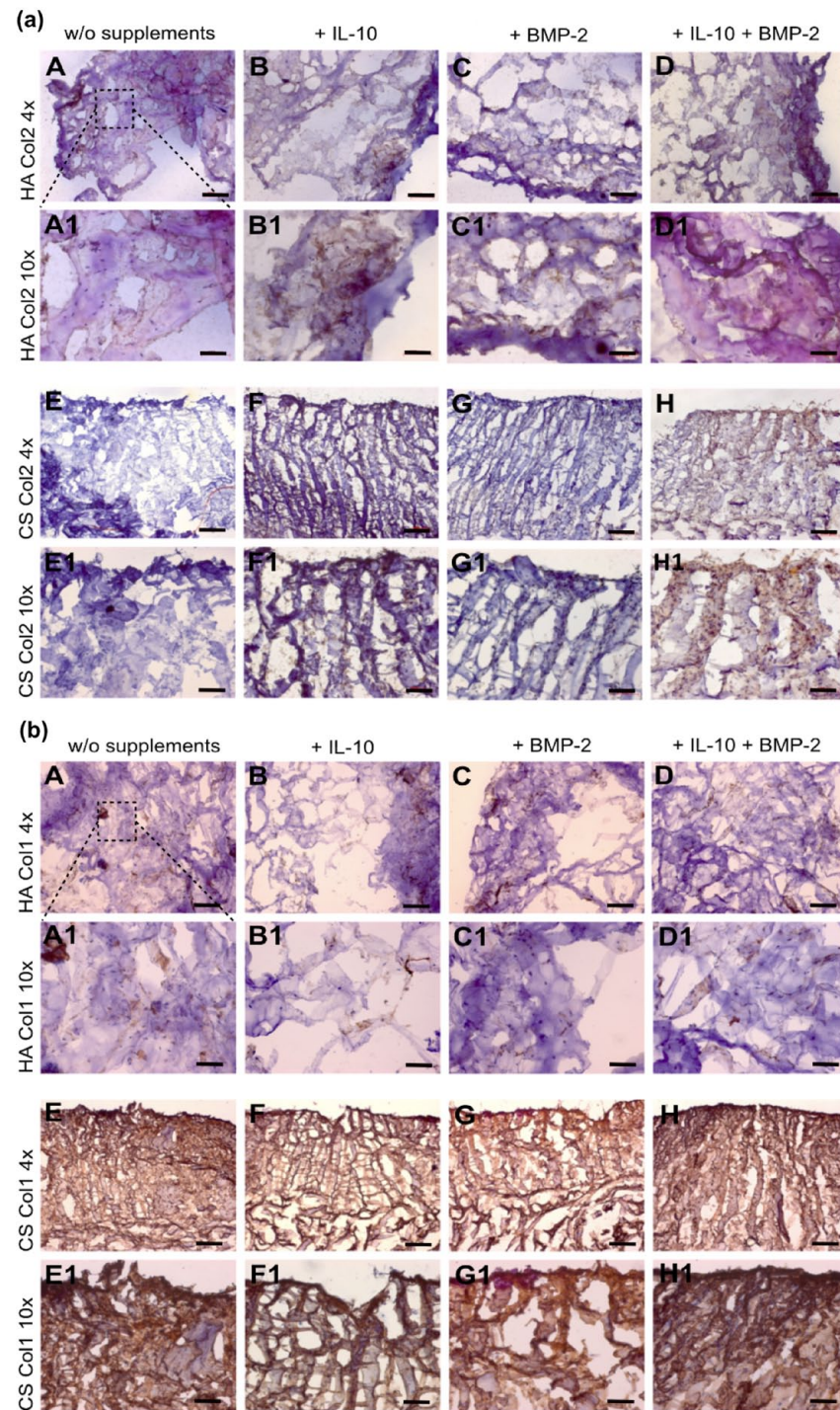


**Figure 4.** (a) Type 2 collagen biosynthesis in cellularized HA (A-D) and CS (E-H). Representative images of type 2 collagen immunohistochemistry after 28 days of culture in chondropermissive medium with and without IL-10 and BMP-2 supplementation (brownish staining indicating type 2 collagen). (b) Type 1 collagen biosynthesis in cellularized HA (A-D) and CS (E-H). Representative images of type 1 collagen immunohistochemistry after 28 days of *in vitro* culture in chondropermissive medium with and without IL-10 and BMP-2 supplementation (brownish staining indicating type 1 collagen) (a and b). HA = hyaluronic acid-based hydrogel; CS = collagen scaffold; ColI = type I collagen; IL-10 = interleukin-10; BMP-2 = bone morphogenetic protein-2; ColII = type 2 collagen. Bar 200 μm (A1-D1, E1-H1: 100 μm).



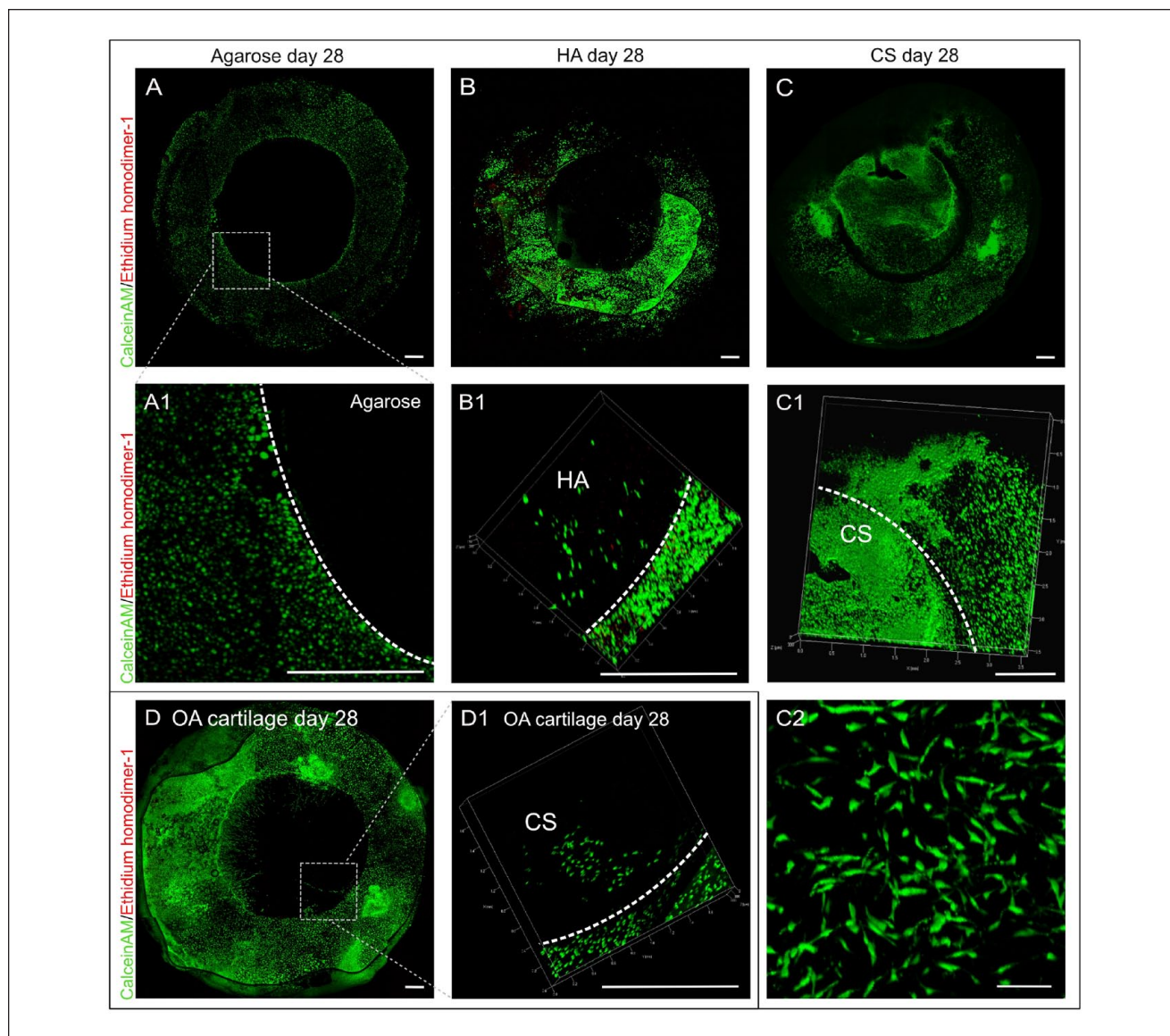


**Figure 5.** Live/dead images of cell invasion assay. (A–C) Representative tile scans after L/D staining of bovine cartilage rings with agarose (negative control), HA and CS embedded after 28 days *in vitro* culture in chondropermissive medium. (A1–C1) Higher magnifications of the biomaterial/cartilage interface. (C2) Morphology of bovine chondrocytes after invasion into CS. (D and D1) Cellular invasion into CS from human osteoarthritic articular cartilage. Bar (A–D) 1 mm, (C2) 100  $\mu$ m. HA = hyaluronic acid-based hydrogel; CS = collagen scaffold; OA cartilage = osteoarthritic cartilage.

In summary, hCh encapsulated in the HA showed favorable chondrogenic phenotype alterations, which was paralleled by chondrocyte morphology as previously observed.

### Deposition of Cartilage-Specific ECM Is Enhanced in CSs

Quantification of sGAG in digested scaffolds normalized to DNA content revealed higher sGAG synthesis in HA in all treatment groups without reaching statistical significance (Fig. 3a(A)). DNA content in HA samples was generally lower

in all groups (HA + BMP-2 vs. CS + BMP-2;  $P = 0.0232$ ; Figure 3a(B)). There was a trend for higher sGAG content in IL-10 and BMP-2-treated samples with pronounced increase in biosynthesis in the co-treatment group (Fig. 3a(C)).

sGAG loss in the medium was less pronounced in CS groups, which was paralleled by higher amount of retained sGAG in CS groups, observed in histology studies (Fig. 3b(A–H)). Toluidine blue staining of HA and CS showed more enhanced metachromasia within the CS grafts with BMP-2 treatment and co-treatment (Fig. 3b(G and H)). No distinct effects of IL-10 were detected. A similar staining

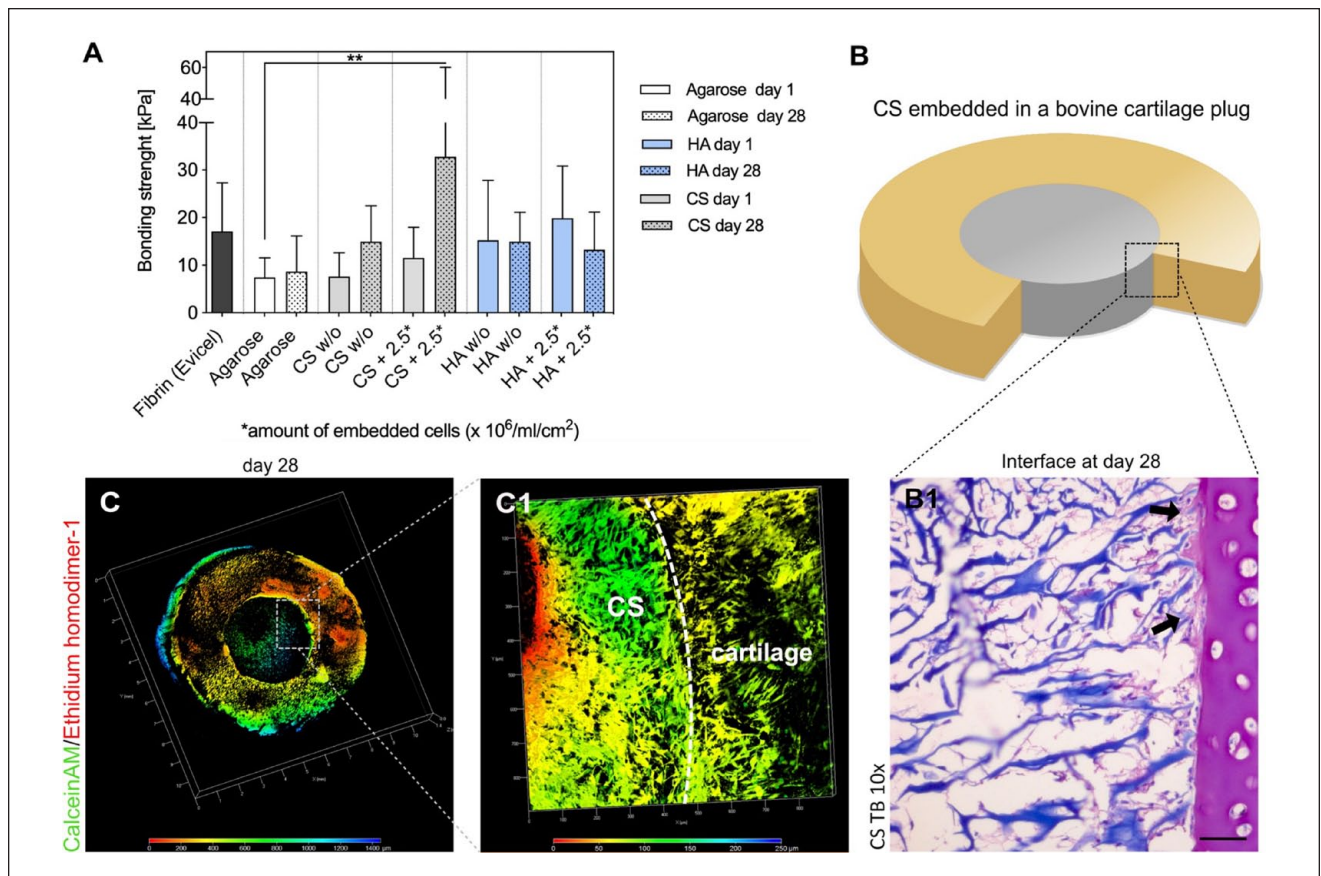


**Figure 6.** Bonding strength of HA and CS to articular cartilage. **(A)** Quantification of bonding strength to articular cartilage of cell-free and cell-laden HA and CS. Asterisks indicate significant differences with  $*P < 0.05$ ,  $**P < 0.01$ , one-way ANOVA. Data are presented as mean  $\pm$  SD ( $n = 6$ ). Agarose served as negative control, fibrin glue served as positive control. **(B)** Representative images of cartilage-CS interface stained with toluidine blue (**B1**) and before push-out testing. **(C)** Depth-coding tile scan of cell-laden CS embedded in bovine cartilage ring with a representative image of the interface (**C1** magnification of the cartilage/CS interface area). Bars (**B** and **D**) 50  $\mu$ m. HA = hyaluronic acid-based hydrogel; CS = collagen scaffold; ANOVA = analysis of variance; SD = standard deviation.

pattern was observed for COL2A1 in IHC (**Fig. 4a(A-H)**). Distinct staining was observed in the same treatment groups as before (**Fig. 4a(G and H)**), but especially the combination of IL-10 and BMP-2 led to significant COL2A1 deposition. Particularly, the application of BMP-2 promoted the deposition of ECM. Positive staining of sGAG and COL2A1 was mainly located on the cell-seeding site of CS. IHC staining of COL1A1 showed minor accumulations in HA groups (**Fig. 4b(A-D)**). As the CS consisted mainly of COL1A1, the staining for COL1A1 was disregarded.

Summarizing, on a histological level, the synthesis of sGAG and its release was higher in HA while chondrocytes embedded in the CS showed markedly enhanced ECM synthesis under the treatment with BMP-2.

#### Cell Invasion Properties of Hydrogel Are Inferior Compared with CS

CLSM imaging revealed high cell invasion into CS (**Fig. 5**). After 28 days, CS explants were almost completely

colonized ( $93.16\% \pm 7.36\%$ ) by bovine chondrocytes through all depths (**Fig. 5(C)**). Similar results have also been observed for human osteoarthritic cartilage (**Fig 5(D)**). In contrast, almost no cell invasion was detected into HA ( $9.33\% \pm 4.41\%$ ; **Figure 5(B)**), and there was no invasion into agarose (0%; **Fig. 5(A)**).

In addition, it was observed that migrating chondrocytes underwent morphological changes. Chondrocytes that colonized CS scaffolds showed a ramified phenotype.

#### Graft Integration of CS Is Superior and in Biomaterial Stiffness Indicates Matrix Deposition

Cellularized HA resulted in a higher initial bonding strength (HA + hCh day 0:  $19.86 \pm 10.96$  kPa; CS without hCh day 0:  $7.12 \pm 4.95$  kPa; CS + hCh day 0:  $11.5 \pm 6.46$  kPa; agarose day 0:  $7.35 \pm 4.12$  kPa; **Figure 6(A)**) compared with agarose and CS grafts, but no significant difference was detected when compared with fibrin glue ( $17.11 \pm 10.2$  kPa). Bonding strength improved over time in all

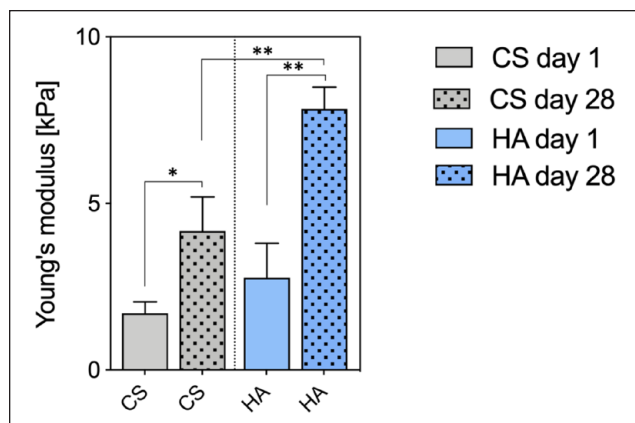


**Figure 7.** Young's modulus of cell-laden biomaterials. Quantification of changes in biomaterial stiffness in cell-laden HA and CS after 28 days compared with day 1. Asterisks indicate significant differences with \* $P < 0.05$ , \*\* $P < 0.01$ , one-way ANOVA. Data are presented as mean + SD ( $n = 3$ ). HA = hyaluronic acid-based hydrogel; CS = collagen scaffold; ANOVA = analysis of variance; SD = standard deviation.

experimental groups except cellularized HA. Highest increase was observed in cellularized CS (CS + hCh day 28:  $32.76 \pm 27.36$  kPa vs. agarose day 0:  $7.35 \pm 4.12$  kPa;  $P = 0.0032$ ). Bonding strength of cell-free hydrogels did not differ significantly at day 28 from initial measurements.

In cellularized CS increasing bonding strength was paralleled by matrix deposition indicating interface maturation (Fig. 6(B1)). Neosynthesis of sGAG was detected adjacent to the cartilage cutting surface and collagen fibers, but also surrounding cell clusters. In addition, macroscopical analysis of the cartilage/HA interface revealed partial detachment after 28 days of culture.

Initial Young's modulus (CS day 1:  $1.7 \pm 0.35$  kPa vs. CS day 28:  $4.17 \pm 1.03$  kPa;  $P = 0.0375$ ; HA day 1:  $2.77 \pm 1.04$  kPa vs. CS day: 28  $7.83 \pm 0.67$  kPa,  $P = 0.0004$ ) significantly increased after 28 days in both biomaterials indicating matrix deposition (Fig. 7). Final Young's modulus of HA was significantly higher compared with CS ( $P = 0.0036$ ).

## Discussion

Many different biomaterials have been proposed in pre-clinical studies to be used in cartilage tissue engineering, but clinical data and comparative analyses are rare. By deepening the knowledge about clinically established ACI products, this study aimed to help future biomaterial development and set a benchmark for new generation technologies.<sup>24</sup>

Our study revealed significant differences of 2 biomaterials used for ACI manufacturing, which can help future tissue engineering and biomaterials science to approach the challenge of articular cartilage repair and regeneration.

The collagen membrane showed distinct advantages in cell colonization and extracellular matrix retention as well as structural integration into native cartilage tissue, while chondrocytes in hydrogels displayed a cell morphology reminiscent of that in hyaline cartilage with a corresponding positive influence on cell differentiation. Administration of BMP-2 during cultivation significantly enhanced chondrogenic differentiation, while IL-10 was less effective. Regarding matrix neosynthesis, the combinatory treatment with both adjuvants revealed synergistic effects.

As expected from clinically applied products, both biomaterials showed a high viability of embedded chondrocytes. In support, hyaluronic acid and CSs have been identified to be ideal biomaterials regarding biocompatibility in numerous studies.<sup>25-27</sup> In this study, higher cell numbers were observed in collagen matrices and this effect was most likely supported by the lack of extracellular binding motives for hChs in HA because it is known that chondrocytes proliferate faster in the presence of structures with extracellular binding motives.<sup>28</sup> A potential mechanism behind this is the binding of chondrocyte integrins to tripeptide Arg-Gly-Asp (RGD) sequences of collagen fibers.<sup>29,30</sup> In this context, the lack of cellular binding motives incorporated in HA seems to slow proliferation. Instead, the cells must synthesize their own extracellular matrix to proliferate and achieve full scaffold colonization. As a potential result of the initially provided biomaterial matrix, the phenotype of the encapsulated chondrocytes also differed. In the gel-based biomaterial, hCh maintained a spherical phenotype similar to that of chondrocytes in hyaline cartilage, while the chondrocytes in the collagen matrix displayed a more ramified phenotype and accumulated F-actin. It is known that chondrocytes adopt a spherical phenotype when embedded in gels although they have been expanded into monolayers beforehand.<sup>31-33</sup> Such differences in the morphological phenotype in turn correlate with the functional cell phenotype.<sup>34,35</sup> The morphological appearance correlated with an increased COL2A1, COL2A1/COL1A1 ratio, and ACAN mRNA expression in the HA compared with the CS, which was consistent in all experimental groups. Type 2 collagen expression at the time of ACI implantation has been identified to correlate with improved clinical outcome data at a 24-month follow-up indicating the relevance of the used biomaterial.<sup>36</sup> The expression of chondrogenic mRNA markers was paralleled by increased GAG neosynthesis per cell and collagen type 2 expression. However, the total amount of sGAG and type 2 collagen staining was more distinct within the CS. By supplementing IL-10 and BMP-2, mRNA expression levels of these markers were increased significantly indicating a positive pre-conditioning effect in the process of ACI manufacturing. Although the effect of IL-10 was less pronounced compared with BMP-2, it may exert additional beneficial effects post ACI implantation. Given the catabolic and proinflammatory micro-environment



following a joint trauma, IL-10 was shown recently to antagonize certain mechanisms of post-traumatic cartilage degeneration.<sup>14,18,37</sup> Therefore, BMP-2 is an interesting candidate to support chondrocyte re-differentiation during the ACI manufacturing process while IL-10 is promising to be used as a post-implantation factor to immune-modulate the post-traumatic joint environment. However, this approach requires post-implantation cytokine release as proposed by different study groups.<sup>38,39</sup> Another factor for advantageous chondrogenic differentiation in HA might be the hyaluronic acid in the biomaterial itself. The hyaluronic acid is passively immobilized in a maleolyl-albumin network cross-linked by PEG and may therefore interact particularly well with the embedded cells. It is known that hyaluronic acid with a lower molecular weight positively influences the joint environment.<sup>8,40</sup> Interestingly, a recent comparative clinical study that examined both ACI types as used in this experimental study revealed accelerated improvement in the clinical IKDC (International Knee Documentation Committee) score for the hydrogel-based ACI, but equivalent clinical results at 2 years follow-up.<sup>41</sup> There is evidence that the biomechanical and ultra-structural properties, which can be assessed by MRI correlate with clinical IKDC score.<sup>42</sup> A recent prospective clinical trial reported high MOCART (Magnetic Resonance Observation of Cartilage Repair Tissue) score up to 80 points for hyaluronic acid-based ACI as used in this study in comparison with previously reported ACI products indicating superior regenerative tissue.<sup>43</sup> Therefore, the reported clinical results may reflect a superior chondrogenic graft maturation as seen in our laboratory study.

Graft integration is another crucial aspect of successful ACI treatment, while vertical integration with the subchondral bone is commonly obtained, lateral integration is still an issue in chondral repair.<sup>44-46</sup> It is likely that cell invasion is an important mechanism to improve graft integration at the defect site. On the contrary, primary bioadhesive properties may be favorable for successful ACI integration and mechanically induced graft maturation. Our study shows that matrices-based biomaterials acquire superior graft integration properties compared with hydrogels in an *ex vivo* organ culture model, which is likely due to marked chondrocyte migration from native cartilage tissue into CSs as well as ECM deposition at the graft/tissue interface as observed in our histology studies.<sup>47</sup> The biomechanical analysis of the lateral integration using a push-out test underlined these results for both cell-free and cellularized biomaterials. Reliable graft incorporation is crucial for ACI application, as graft delamination is a major reason for ACI failure.<sup>48</sup> Clinically, no delamination has been reported for the HA.<sup>43</sup> In addition, strong graft incorporation may allow early weightbearing, which is crucial to allow for mechano-induced chondrocyte differentiation.<sup>23</sup> Mechanotransduction is an important mechanism of graft maturation.<sup>23,34,35,49,50</sup>

Considering the *in vivo* situation, a higher initial primary stiffness might be advantageous for graft healing. Without the addition of exogenous growth factors, Behrendt *et al.*<sup>23</sup> showed recently that one of the most potent tissue factors, TGF- $\beta$ , is produced and activated by mechanical load, which can significantly accelerate graft maturation and subsequently lead to improved cartilage regeneration. As both biomaterials have a rather low Young's modulus even after 28 days of culture, a hybrid scaffold that combines both material properties may be favorable in future developments. Importantly, an essential advantage of hydrogels is the versatile tuneability of its biomechanical properties like matrix stiffness, cross-linking density, and stress relaxation, which also affect chondrocyte differentiation.<sup>49,50</sup>

However, the impact of migrating cells on the transplanted cells within the biomaterial is not fully understood.<sup>45</sup> As CLSM imaging in our study revealed, the hCh that migrated into the biomaterial displayed a ramified phenotype similar to the ones that underwent monolayer expansion. In addition, cell migration from the subchondral bone *in vivo* may occur, which could be one disadvantage of 3-dimensional matrices due to the inferior regenerative potential of bone marrow precursor cells, which in turn leads to biological and biomechanical inferior fibrocartilage tissue rich in type I collagen.<sup>51</sup>

This study has some relevant limitations due to the *in vitro* study design and usage of hip OA chondrocytes. OA chondrocytes have known age-dependent proliferation and differentiation capacities, which limits the translational interpretation of the results.<sup>52,53</sup> Several *in vivo* influences cannot be mimicked *in vitro* such as the joint environment, which will differ from the culture media used in this study.

## Conclusion

Cell-biomaterial interactions enable distinct advantages for chondrocyte re-differentiation and cartilage formation. None of both biomaterials have been superior to one another, but both revealed different advantages with respect to cell differentiation, matrix retention, graft integration strength, cellularity, and cell migration. Hybrid constructs taking advantage of different biomaterial advantages as well as soluble adjuvants to control degenerative or post-traumatic micro-environment might be the future of further ACI development.

## Author Contributions

Conceptualization: J.-T.W., S.L., B.K., P.B.; Methodology: J.-T.W., K.B., B.K., P.B.; Validation: J.-T.W., K.B., R.L., B.K., P.B.; Formal analysis: J.-T.W., P.B.; Investigation: J.-T.W., B.R., A.B., M.W., H.N., J.W., M.H., S.L., B.K., P.B.; Writing—original draft preparation: J.-T.W., K.B., B.K., P.B.; Writing—review and editing: all authors; Visualization: J.-T.W.; Supervision: B.K.; Project

administration: R.L.; Funding acquisition: B.K., P.B. All authors have read and approved the final version of this manuscript.

### Acknowledgments and Funding

The authors thank Rita Kirsch and Frank Lichte for their excellent technical assistance. The author(s) disclosed receipt of the following financial support for the research, authorship, and/or publication of this article: This research project was funded the Faculty of Medicine at the Kiel University. Collagen scaffolds and hydrogel components were provided by TETEC Tissue Engineering Technologies AG, Reutlingen, Germany. We acknowledge financial support by Land Schleswig-Holstein within the funding programs Open Access Publikationsfonds.

### Declaration of Conflicting Interests

The author(s) declared the following potential conflicts of interest with respect to the research, authorship, and/or publication of this article: The authors declare no conflict of interest. PB and MH declare that the clinical products investigated in this study are clinically used by PB and MH. KB is head of the research and development department of TETEC Tissue Engineering Technologies AG. KB had no role in the design of the study; in the collection, analyses, or interpretation of data; or in the decision to publish the results.

### Ethical Approval

Ethical approval for the present study was obtained of Kiel University (D572/17).

### ORCID iD

Jan-Tobias Weitkamp  <https://orcid.org/0000-0002-0242-0784>

### References

1. Brittberg M, Lindahl A, Nilsson A, Ohlsson C, Isaksson O, Peterson L. Treatment of deep cartilage defects in the knee with autologous chondrocyte transplantation. *N Engl J Med*. 1994 Oct 6;331(14):889-95. doi:10.1056/nejm199410063311401.
2. Niemeyer P, Albrecht D, Andereya S, Angele P, Ateschrang A, Aurich M, *et al*. Autologous chondrocyte implantation (ACI) for cartilage defects of the knee: a guideline by the working group "Clinical Tissue Regeneration" of the German Society of Orthopaedics and Trauma (DGOU). *Knee*. 2016 Jun;23(3):426-35. doi:10.1016/j.knee.2016.02.001.
3. Gooding CR, Bartlett W, Bentley G, Skinner JA, Carrington R, Flanagan A. A prospective, randomised study comparing two techniques of autologous chondrocyte implantation for osteochondral defects in the knee: periosteum covered versus type I/III collagen covered. *Knee*. 2006 Jun;13(3):203-10. doi:10.1016/j.knee.2006.02.011.
4. Harris JD, Siston RA, Pan X, Flanagan DC. Autologous chondrocyte implantation: a systematic review. *J Bone Joint Surg Am Vol*. 2010 Sep 15;92(12):2220-33. doi:10.2106/jbjs.J.00049.
5. Benya PD, Padilla SR, Nimni ME. Independent regulation of collagen types by chondrocytes during the loss of differentiated function in culture. *Cell*. 1978 Dec;15(4):1313-21. doi:10.1016/0092-8674(78)90056-9.
6. Niemeyer P, Salzmann G, Feucht M, Pestka J, Porichis S, Ogon P, *et al*. First-generation versus second-generation autologous chondrocyte implantation for treatment of cartilage defects of the knee: a matched-pair analysis on long-term clinical outcome. *Int Orthop*. 2014 Oct;38(10):2065-70. doi:10.1007/s00264-014-2368-0.
7. Yoo HS, Lee EA, Yoon JJ, Park TG. Hyaluronic acid modified biodegradable scaffolds for cartilage tissue engineering. *Biomaterials*. 2005 May;26(14):1925-33. doi:10.1016/j.biomaterials.2004.06.021.
8. Ehlers EM, Behrens P, Wünsch L, Kühnel W, Russlies M. Effects of hyaluronic acid on the morphology and proliferation of human chondrocytes in primary cell culture. *Ann Anat*. 2001 Jan;183(1):13-7. doi:10.1016/s0940-9602(01)80007-8.
9. Irawan V, Sung TC, Higuchi A, Ikoma T. Collagen scaffolds in cartilage tissue engineering and relevant approaches for future development. *Tissue Eng Regen Med*. 2018 Dec;15(6):673-97. doi:10.1007/s13770-018-0135-9.
10. Nuernberger S, Cyran N, Albrecht C, Redl H, Vécsei V, Marlovits S. The influence of scaffold architecture on chondrocyte distribution and behavior in matrix-associated chondrocyte transplantation grafts. *Biomaterials*. 2011;32(4):1032-40. doi:10.1016/j.biomaterials.2010.08.100.
11. Calabrese G, Gulino R, Giuffrida R, Forte S, Figallo E, Fabbì C, *et al*. In vivo evaluation of biocompatibility and chondrogenic potential of a cell-free collagen-based scaffold. *Front Physiol*. 2017;8:984. doi:10.3389/fphys.2017.00984.
12. Wei W, Ma Y, Yao X, Zhou W, Wang X, Li C, *et al*. Advanced hydrogels for the repair of cartilage defects and regeneration. *Bioact Mater*. 2021 Apr;6(4):998-1011. doi:10.1016/j.bioactmat.2020.09.030.
13. Karin Benz CF, Müller J, Wurst H, Albrecht D, Badke A, Gaissmaier C, *et al*. A polyethylene glycol-crosslinked serum albumin/hyaluronan hydrogel for the cultivation of chondrogenic cell types. *Adv Eng Mater*. 2010;12(9):B539-51. doi:10.1002/adem.201080028.
14. Behrendt P, Feldheim M, Preusse-Prange A, Weitkamp JT, Haake M, Eglin D, *et al*. Chondrogenic potential of IL-10 in mechanically injured cartilage and cellularized collagen ACI grafts. *Osteoarthritis Cartilage*. 2018 Feb;26(2):264-75. doi:10.1016/j.joca.2017.11.007.
15. Albrecht C, Schlegel W, Bartko P, Eckl P, Jagersberger T, Vecsei V, *et al*. Changes in the endogenous BMP expression during redifferentiation of chondrocytes in 3D cultures. *Int J Mol Med*. 2010 Sep;26(3):317-23.
16. Schulze-Tanzil G, Zreiqat H, Sabat R, Kohl B, Halder A, Müller RD, *et al*. Interleukin-10 and articular cartilage: experimental therapeutic approaches in cartilage disorders. *Curr Gene Ther*. 2009 Aug;9(4):306-15. doi:10.2174/156652309788921044.
17. Müller RD, John T, Kohl B, Oberholzer A, Gust T, Hostmann A, *et al*. IL-10 overexpression differentially affects cartilage matrix gene expression in response to TNF-alpha in human articular chondrocytes in vitro. *Cytokine*. 2008 Dec;44(3):377-85. doi:10.1016/j.cyto.2008.10.012.
18. Weitkamp JT, Rolaußs B, Feldheim M, Bayer A, Lippross S, Weuster M, *et al*. Regenerative potential of platelet concentrate lysate in mechanically injured cartilage and matrix-

- associated chondrocyte implantation in vitro. *Int J Mol Sci.* 2021 Dec 7;22(24):13179. doi:10.3390/ijms222413179.
19. Zheng CH, Levenston ME. Fact versus artifact: avoiding erroneous estimates of sulfated glycosaminoglycan content using the dimethylmethylene blue colorimetric assay for tissue-engineered constructs. *Eur Cell Mater.* 2015 Apr 19;29:224-36; discussion 236.
  20. Loening AM, James IE, Levenston ME, Badger AM, Frank EH, Kurz B, *et al.* Injurious mechanical compression of bovine articular cartilage induces chondrocyte apoptosis. *Arch Biochem Biophys.* 2000 Sep 15;381(2):205-12. doi:10.1006/abbi.2000.1988.
  21. Gille J, Kunow J, Boisch L, Behrens P, Bos I, Hoffmann C, *et al.* Cell-laden and cell-free matrix-induced chondrogenesis versus microfracture for the treatment of articular cartilage defects: a histological and biomechanical study in sheep. *Cartilage.* 2010 Jan;1(1):29-42. doi:10.1177/1947603509358721.
  22. Kurz B, Domm C, Jin M, Selckau R, Schünke M. Tissue engineering of articular cartilage under the influence of collagen I/III membranes and low oxygen tension. *Tissue Eng.* 2004 Jul-Aug;10(7-8):1277-86. doi:10.1089/ten.2004.10.1796.
  23. Behrendt P, Ladner Y, Stoddart MJ, Lippross S, Alini M, Eglin D, *et al.* Articular joint-simulating mechanical load activates endogenous TGF-beta in a highly cellularized bioadhesive hydrogel for cartilage repair. *Am J Sports Med.* 2020 Jan;48(1):210-21. doi:10.1177/0363546519887909.
  24. Armiento AR, Stoddart MJ, Alini M, Eglin D. Biomaterials for articular cartilage tissue engineering: learning from biology. *Acta Biomater.* 2018 Jan;65:1-20. doi:10.1016/j.actbio.2017.11.021.
  25. Willers C, Chen J, Wood D, Xu J, Zheng MH. Autologous chondrocyte implantation with collagen bioscaffold for the treatment of osteochondral defects in rabbits. *Tissue Eng.* 2005 Jul-Aug;11(7-8):1065-76. doi:10.1089/ten.2005.11.1065.
  26. Chircov C, Grumezescu AM, Bejenaru LE. Hyaluronic acid-based scaffolds for tissue engineering. *Rom J Morphol Embryol.* 2018;59(1):71-6.
  27. Cen L, Liu W, Cui L, Zhang W, Cao Y. Collagen tissue engineering: development of novel biomaterials and applications. *Pediatr Res.* 2008 May;63(5):492-6. doi:10.1203/PDR.0b013e31816c5bc3.
  28. Cavalcanti-Adam EA, Volberg T, Micoulet A, Kessler H, Geiger B, Spatz JP. Cell spreading and focal adhesion dynamics are regulated by spacing of integrin ligands. *Biophys J.* 2007 Apr 15;92(8):2964-74. doi:10.1529/biophysj.106.089730.
  29. Ruoslahti E. RGD and other recognition sequences for integrins. *Annu Rev Cell Dev Biol.* 1996;12:697-715. doi:10.1146/annurev.cellbio.12.1.697.
  30. Yang M, Zhang ZC, Liu Y, Chen YR, Deng RH, Zhang ZN, *et al.* Function and mechanism of RGD in Bone and cartilage tissue engineering. *Front Bioeng Biotechnol.* 2021;9:773636. doi:10.3389/fbioe.2021.773636.
  31. Benya P. Dedifferentiated chondrocytes reexpress the differentiated collagen phenotype when cultured in agarose gels. *Cell.* 1982;30(1):215-24. doi:10.1016/0092-8674(82)90027-7.
  32. Kimura T, Yasui N, Ohsawa S, Ono K. Chondrocytes embedded in collagen gels maintain cartilage phenotype during long-term cultures. *Clin Orthop Relat Res.* 1984 Jun;186:231-9.
  33. Takahashi T, Ogasawara T, Asawa Y, Mori Y, Uchinuma E, Takato T, *et al.* Three-dimensional microenvironments retain chondrocyte phenotypes during proliferation culture. *Tissue Eng.* 2007 Jul;13(7):1583-92. doi:10.1089/ten.2006.0322.
  34. Lauer JC, Selig M, Hart ML, Kurz B, Rolauffs B. Articular chondrocyte phenotype regulation through the cytoskeleton and the signaling processes that originate from or converge on the cytoskeleton: towards a novel understanding of the intersection between actin dynamics and chondrogenic function. *Int J Mol Sci.* 2021 Mar 23;22(6):3279. doi:10.3390/ijms22063279.
  35. Selig M, Lauer JC, Hart ML, Rolauffs B. Mechanotransduction and stiffness-sensing: mechanisms and opportunities to control multiple molecular aspects of cell phenotype as a design cornerstone of cell-instructive biomaterials for articular cartilage repair. *Int J Mol Sci.* 2020 Jul 29;21(15):5399. doi:10.3390/ijms21155399.
  36. Niemeyer P, Pestka JM, Salzmann GM, Südkamp NP, Schmal H. Influence of cell quality on clinical outcome after autologous chondrocyte implantation. *Am J Sports Med.* 2012 Mar;40(3):556-61. doi:10.1177/0363546511428879.
  37. Behrendt P, Preusse-Prange A, Kluter T, Haake M, Rolauffs B, Grodzinsky AJ, *et al.* IL-10 reduces apoptosis and extracellular matrix degradation after injurious compression of mature articular cartilage. *Osteoarthritis Cartilage.* 2016 Nov;24(11):1981-8. doi:10.1016/j.joca.2016.06.016.
  38. Evenbratt H, Andreasson L, Bicknell V, Brittberg M, Mobini R, Simonsson S. Insights into the present and future of cartilage regeneration and joint repair. *Cell Regen.* 2022 Feb 2;11(1):3. doi:10.1186/s13619-021-00104-5.
  39. Park E, Hart ML, Rolauffs B, Stegemann JP, Annamalai RT. Bioresponsive microspheres for on-demand delivery of anti-inflammatory cytokines for articular cartilage repair. *J Biomed Mater Res A.* 2020 Mar;108(3):722-33. doi:10.1002/jbm.a.36852.
  40. Julovi SM, Ito H, Nishitani K, Jackson CJ, Nakamura T. Hyaluronan inhibits matrix metalloproteinase-13 in human arthritic chondrocytes via CD44 and P38. *J Orthop Res.* 2011 Feb;29(2):258-64. doi:10.1002/jor.21216.
  41. Niethammer TR, Uhlemann F, Zhang A, Holzgruber M, Wagner F, Müller PE. Hydrogel-based autologous chondrocyte implantation leads to subjective improvement levels comparable to scaffold based autologous chondrocyte implantation. *Knee Surg Sports Traumatol Arthrosc.* 2022 Feb 28;30(10):3386-92. doi:10.1007/s00167-022-06886-8.
  42. Goller SS, Heuck A, Erber B, Fink N, Rückel J, Niethammer TR, *et al.* Magnetic resonance observation of cartilage repair tissue (MOCART) 2.0 for the evaluation of retropatellar autologous chondrocyte transplantation and correlation to clinical outcome. *Knee.* 2022 Jan;34:42-54. doi:10.1016/j.knee.2021.11.003.
  43. Niemeyer P, Hanus M, Belickas J, László T, Gudas R, Fiodorovas M, *et al.* Treatment of large cartilage defects in the knee by hydrogel-based autologous chondrocyte implantation: two-year results of a prospective, multicenter, single-arm phase III trial. *Cartilage.* 2022 Jan-Mar;13(1):19476035221085146. doi:10.1177/19476035221085146.
  44. Dhollander A, Verdonk P, Tirico LEP, Gomoll AH. Treatment of failed cartilage repair: state of the art. *J ISAKOS.* 2016;1:338-46. doi:10.1136/jisakos-2016-000057.



45. Qu F, Guilak F, Mauck RL. Cell migration: implications for repair and regeneration in joint disease. *Nat Rev Rheumatol*. 2019 Mar;15(3):167-79. doi:10.1038/s41584-018-0151-0.
46. Morales TI. Chondrocyte moves: clever strategies? *Osteoarthritis Cartilage*. 2007 Aug;15(8):861-71. doi:10.1016/j.joca.2007.02.022.
47. Pabbruwe MB, Esfandiari E, Kafienah W, Tarlton JF, Hollander AP. Induction of cartilage integration by a chondrocyte/collagen-scaffold implant. *Biomaterials*. 2009 Sep;30(26):4277-86. doi:10.1016/j.biomaterials.2009.02.052.
48. Harris JD, Siston RA, Brophy RH, Lattermann C, Carey JL, Flanigan DC. Failures, re-operations, and complications after autologous chondrocyte implantation—a systematic review. *Osteoarthritis Cartilage*. 2011 Jul;19(7):779-91. doi:10.1016/j.joca.2011.02.010.
49. Toh WS, Lim TC, Kurisawa M, Spector M. Modulation of mesenchymal stem cell chondrogenesis in a tunable hyaluronic acid hydrogel microenvironment. *Biomaterials*. 2012 May;33(15):3835-45. doi:10.1016/j.biomaterials.2012.01.065.
50. Lee HP, Gu L, Mooney DJ, Levenston ME, Chaudhuri O. Mechanical confinement regulates cartilage matrix formation by chondrocytes. *Nat Mater*. 2017 Dec;16(12):1243-51. doi:10.1038/nmat4993.
51. Knutsen GE, Ngebreetsen L, Ludvigsen TC, Drogset JO, Grøntvedt T, Solheim E, *et al*. Autologous chondrocyte implantation compared with microfracture in the knee. A randomized trial. *J Bone Joint Surg Am*. 2004;86(3):455-64. doi:10.2106/00004623-200403000-00001.
52. Tallheden T, Bengtsson C, Brantsing C, Sjogren-Jansson E, Carlsson L, Peterson L, *et al*. Proliferation and differentiation potential of chondrocytes from osteoarthritic patients. *Arthritis Res Ther*. 2005 Mar;7(3):R560-158. doi:10.1186/ar1709.
53. Bulstra SK, Buurman WA, Walenkamp GH, Van der Linden AJ. Metabolic characteristics of in vitro cultured human chondrocytes in relation to the histopathologic grade of osteoarthritis. *Clin Orthop Relat Res*. 1989 May;242:294-302.